Xu et al. Journal of Inflammation (2024) 21:47
https://doi.org/10.1186/s12950-024-00411-z

Journal of Inflammation

RESEARCH Open Access

Carvacrol alleviates LPS-induced myocardial dysfunction by inhibiting the TLR4/MyD88/NF-κB and NLRP3 inflammasome in cardiomyocytes

Lu Xu[1], Xu Yang[1], Xiao-Ting Liu[1], Xia-Yun Li[1], Han-Zhao Zhu[2], Yan-Hua Xie[1], Si-Wang Wang[1*], Yao Li[3*] and Ye Zhao[1*]

Abstract

Background Sepsis-induced myocardial dysfunction (SIMD) may contribute to the poor prognosis of septic patients. Carvacrol (2-methyl-5-isopropyl phenol), a phenolic monoterpene compound extracted from various aromatic plants and fragrance essential oils, has multiple beneficial effects such as antibacterial, anti-inflammatory, and antioxidant properties. These attributes make it potentially useful for treating many diseases. This study aims to investigate the effects of CAR on LPS-induced myocardial dysfunction and explore the underlying mechanism.

Results H9c2 cells were stimulated with 10 μg/ml LPS for 12 h, and c57BL/6 mice were intraperitoneally injected with 10 mg/kg LPS to establish a septic-myocardial injury model. Our results showed that CAR could improve cardiac function, significantly reduce serum levels of inflammatory cytokines (including TNF-α, IL-1β, and IL-6), decrease oxidative stress, and inhibit cardiomyocyte apoptosis in LPS-injured mice. Additionally, CAR significantly downregulated the expression of TLR4, MyD88, and NF-κB in LPS-injured mice and H9c2 cells. It also inhibited the upregulation of inflammasome components (such as NLRP3, GSDMD, and IL-1β) in H9c2 cells triggered by LPS.

Conclusion Taken together, CAR exhibited potential cardioprotective effects against sepsis, which may be mainly attributed to the TLR4/MyD88/NF-κB pathway and the NLRP3 inflammasome.

Keywords Myocardial dysfunction, Lipopolysaccharide (LPS), Carvacrol, Inflammation, Apoptosis

Introduction

Based on the Third International Consensus Definitions for Sepsis and Septic Shock published in 2016, sepsis is defined as "a life-threatening organ dysfunction caused by dysregulated host response to infection" [1]. Sepsis-induced myocardial dysfunction (SIMD) is one of the most common and serious complications of sepsis with a high mortality [2–4]. SIMD is a reversible myocardial dysfunction characterized by decreased myocardial contractility and impaired myocardial compliance, including ventricular dilation and decreased ejection fraction. It is reported that SIMD are responsible for the complicated

*Correspondence:
Si-Wang Wang
wangsiw@nwu.edu.cn
Yao Li
18792768149@163.com
Ye Zhao
zhaoye@nwu.edu.com
[1]The College of Life Science, Northwest University, Xi'an, China
[2]Department of Cardiovascular Surgery, The First Affiliated Hospital, The Air Force Medical University, Xi'an, China
[3]School of Pharmacy, Shaanxi University of Chinese Medicine, Xianyang, China

mechanisms, including inflammatory responses, oxidative stress, calcium disturbances, autophagy, apoptosis, and mitochondrial dysfunction [2, 4, 5]. Despite of numerous pharmacologic and non-pharmacologic treatments that have been applied clinically, there are currently no effective treatments for SIMD, and antibiotic therapy remains the primary treatment approach for managing sepsis in clinical settings [2]. In addition, imipenem exhibits optimal efficacy in control systemic and local inflammation, thereby maintaining all T-lymphocyte populations, reducing liver injury, and ultimately improving survival rates, it represents a promising therapeutic strategy in the management of sepsis [6]. In our study, imipenem was used as a positive drug. Therefore, it is an imperious demand to develop more effective drugs for myocardial dysfunction.

The lipopolysaccharide (LPS), also known as endotoxin, is the main component of the cell wall of Gram-negative bacteria. LPS depresses intrinsic myocardial contractility and is an important factor contributing to myocardial dysfunction during sepsis [7]. LPS binds to the pattern recognition receptors (PRRs) of innate immune cells, which causes the activation of associated downstream signaling pathways and the release of inflammatory mediators (cytokines, such as chemokines, etc.) [8, 9]. Inflammatory cytokine production is regulated by several mechanisms, including TLR4 and its downstream signaling pathways, namely the mitogen-activated protein kinase (MAPK) and nuclear factor κB(NF-κB) pathways. Toll-like receptors of cardiomyocytes, especially TLR4, is the key molecule of myocardial dysfunction in sepsis, and myocardial inhibitory factors represented by TNF-α, IL-6 are also involved in the occurrence and development of SIMD [10]. The NLRP3 inflammasome, as an important component of innate immunity, plays a key role in sepsis and septic myocardial injury, and NLRP3 inflammasome can be activated by a variety of pathogen-associated molecular patterns (PAMPs) [11]. Excessive activation of the NLRP3 inflammasome leads to excessive release of pro-inflammatory factors and massive cell death, resulting in sepsis and multiple organ damage, including myocardial depression, while NLRP3 inhibitor or NLRP3 knock out reduces the systemic inflammatory response and relieves and organ dysfunction [12, 13].

Traditional Chinese medicines have been widely used in the treatment of various diseases. Carvacrol (CAR), also known as 2-methyl-5-isopropylphenol, is a natural polyphenol that is commonly found in the essential oils of aromatic plants such as oregano (*Origanum vulgare*), thyme (*Thymus vulgaris*), pepperwort (*Lepidium flavum*), wild bergamot (*Citrus aurantium bergamia*) and fruits of Ajwain (*Carum copticum*) [14, 15]. CAR has a wide range of pharmacological properties, including antibacterial, antioxidant, anti-inflammatory and analgesic, anti-apoptosis, etc [14, 16–21]. In addition, studies have shown that CAR can protect against a variety of cardiovascular diseases. Previous studies investigating the possible protective effects of CAR against endothelial inflammation in db/db mice. Zhao et al. [22] reported that CAR significantly reduced serum levels of insulin signaling molecules, insulin, total cholesterol, and inflammatory cytokine expression in db/db mice. Several studies have confirmed that CAR had a protective effect against ischemia-reperfusion, protecting cardiac function, reducing infarct size, increasing SOD and CAT levels, decreasing MDA levels, and especially decreasing cardiomyocyte apoptosis [23, 24]. Moreover, Jafarinezhad et al. [25] and El-Sayed et al. [26] demonstrated that CAR mitigates doxorubicin-induced cardiotoxicity by reducing lipid peroxidation, inhibiting TNF-α production, and attenuating apoptotic effects. In particular, the role of CAR in alleviating inflammatory injury through the TLR4 pathway has been validated in several pathological scenarios [19, 27]. However, whether CAR protects mice from LPS-induced septic myocardial injury through the TLR4 pathway has not been reported. In this study, we aim to evaluate the potential effect and mechanism of CAR in SIMD in vivo and in vitro.

Methods

Animals

Adult male C57BL/6 mice (8 to 10 weeks) were obtained from the Experimental Animal Center of the Air Force Medical University (Xi'an, China). All animals were housed in 60% ± 10% relative humidity and 23℃ ± 2℃ temperature room, with 12/12 h light/dark cycle, and were free access to water and food. All the animal experiments procedures were performed with the approval of the Air Force Military Medical University (No. 20191206).

Materials

CAR was obtained from Jishui Junda Natural Flavor Oil Factory (Jiangxi, China). LPS (From Escherichia coli 055:B5) was purchased from Beijing Solarbio Science & Technology Co., Ltd. (Beijing, China). Kits for the detection of creatine kinase MB (CK-MB), lactate dehydrogenase (LDH), cardiac troponin I (cTnI), tumor necrosis factor (TNF-α), interleukin-1β (IL-1β), interleukin-6(IL-6), superoxide dismutase (SOD) and malondialdehyde (MDA) were obtained from Elabscience Biotechnology Co., Ltd (Wuhan, China). Dihydroethidium (DHE) were purchased from Invitrogen (Carlsbad, USA). Primary antibodies against TLR4 (WL00196), MyD88 (WL02494) were purchased from Wanlei Life Sciences Co., Ltd (Shenyang, China). Primary antibodies against JNK (#9252), phospho-JNK (#4668), phospho-p38 (#4092), phospho-NF-κB (#3033), phosphor-IκB (#2859),

IκB (#76041) and GSDMD (#46451) were purchased from Cell Signaling Technology (Boston, USA). Primary antibodies against p-38 (ab170099), NF-κB (ab32536), IL-1β (ab283818), TNF-α (ab215188), Bax (ab32503), Bcl-2 (ab182858), Caspase-3 (ab184787) and GAPDH (ab8245) were purchased from Abcam (Cambridge, USA). Primary antibodies against NLRP3 (27458-1-AP), β-actin (66009-1-Ig), Caspase-1(22915-1-AP), IL-18(60070-1-Ig) were purchased from Proteintech Group (Chicago, USA). The rabbit anti-goat and goat anti-mouse secondary antibodies were obtained from the Zhongshan Company (Beijing, China).

Experimental protocol

To investigate the protective effect of CAR in myocardial injury mice by LPS injection. All experimental animals were randomly divided into six groups Fig. 1(A): normal control (NC) group; LPS group; imipenem (IPM)-treated group (120 mg/kg); low-dose CAR-treated group (25 mg/kg); medium-dose CAR-treated group (50 mg/kg) and high-dose CAR-treated group (100 mg/kg). NC group was no treatments, mice in the CAR groups were gavaged with CAR 25, 50, 100 mg/kg for seven days. Then mice in both the model and CAR groups were intraperitoneally injected with LPS (10 mg/kg) on the seventh day to induced myocardial injury.

Blood samples were collected 12 h after LPS treatment. The serum samples were centrifuged for 15 min at 4000×g centrifugation and stored at -80℃ for further biochemical evaluation. Then, the mice were anesthetized and euthanasia. Heart tissues were perfused with PBS and rapidly dissected stored at -80℃.

Cell culture and treatment

H9c2 cardiomyocyte lines were purchased from Tiancheng Technology (Shanghai, China). Normal control cells were cultured in high-glucose Dulbecco's modified medium (DMEM) (HyClone, Logan, UT, USA) supplemented with 10% fetal bovine serum and 1% penicillin/streptomycin at 37℃ in a humidified atmosphere (5% CO_2). The cell culture medium was replaced with fresh medium containing LPS (10 μg/ml) to induce cardiomyocyte injury model in vitro when the cell density reached about 70%. In addition, the NC group cells were cultured without any treatment, while the LPS-treated cells constituted the model group. Different concentrations of CAR (0.75、1.5、3μM) were added to the culture medium for 6 h, after which the cells were stimulated with LPS. The cells were collected 12 h after LPS stimulation for Western blot analysis.

Echocardiographic assessment

After 12 h of LPS injury, animals were anesthetized with Isoflurane (3% for induction; 1.5–2.5% for maintenance), cardiac function was assessed by Visual-Sonics high resolution Veve 2100 system. All the results were averaged from five consecutive cardiac cycles measuring from the M-mode images. Left ventricular ejection fraction (LVEF) and left ventricular fraction shortening (LVFS) were calculated by computer algorithms.

Detection of myocardial zymogram

The LDH was detected through an automated biochemical analyzer. Serum levels of CK-MB and cTnI (Elabscience Biotechnology Co., Ltd., Wuhan, China) were determined using colorimetric assay, respectively. The assay of LDH, CK-MB and cTnI were performed according to the manufacturer instructions.

Hematoxylin-eosin staining

A standard histological hematoxylin and eosin (HE) staining method was performed. The heart tissue was fixed with 4% paraformaldehyde overnight at 4℃ and embedded in paraffin and sliced into 5 mm for HE staining. The tissue samples were observed under a light microscope.

Determination of cytokine levels

The serum levels of TNF-α, IL-1β and IL-6 was estimated using mouse TNF-α, IL-1β and IL-6 ELISA kit (Elabscience Biotechnology Co., Ltd, Wuhan, China) according to the manufacturer instructions. This is a double-antibody sandwich ELISA method. Samples were diluted and 100 μL of each dilution of standard, blank, and samples was added to the pre-coated 96-well plate. Then 100 μL biotinylated specific antibody immediately added to each well and incubated for 1 h at 37℃. Each well was washed with 350 μL of Wash Solution, followed by the addition of 100 μL HRP Conjugate and incubation for 30 min at 37℃. The wash process was repeated and then 90 μL substrate reagent was added to each well and incubated for10-20 min at 37℃, followed by the addition of 50 μL stop solution and measurement by a microplate reader at 450 nm.

Measurement of oxidative stress

The levels of SOD activity and MDA were determined using SOD and MDA assay kits according to the manufacturer's instructions. For heart tissues, DHE fluorescent probe was used for detecting ROS generation. Frozen sections were fixed with iced acetone at 4℃ for 1 h. The sections were washed with PBS and incubated with 10 μM DHE fluorescent probe for h at 37℃. For H9c2 cells, after 24 h of CAR intervention, DCFH-DA was diluted with serum-free culture medium at 1:1,000 to reach a final concentration of 10 μmol/L, and incubated with the cells for 20 min. The DCFH-DA that had not entered the cells was sufficiently removed. Tissue images were

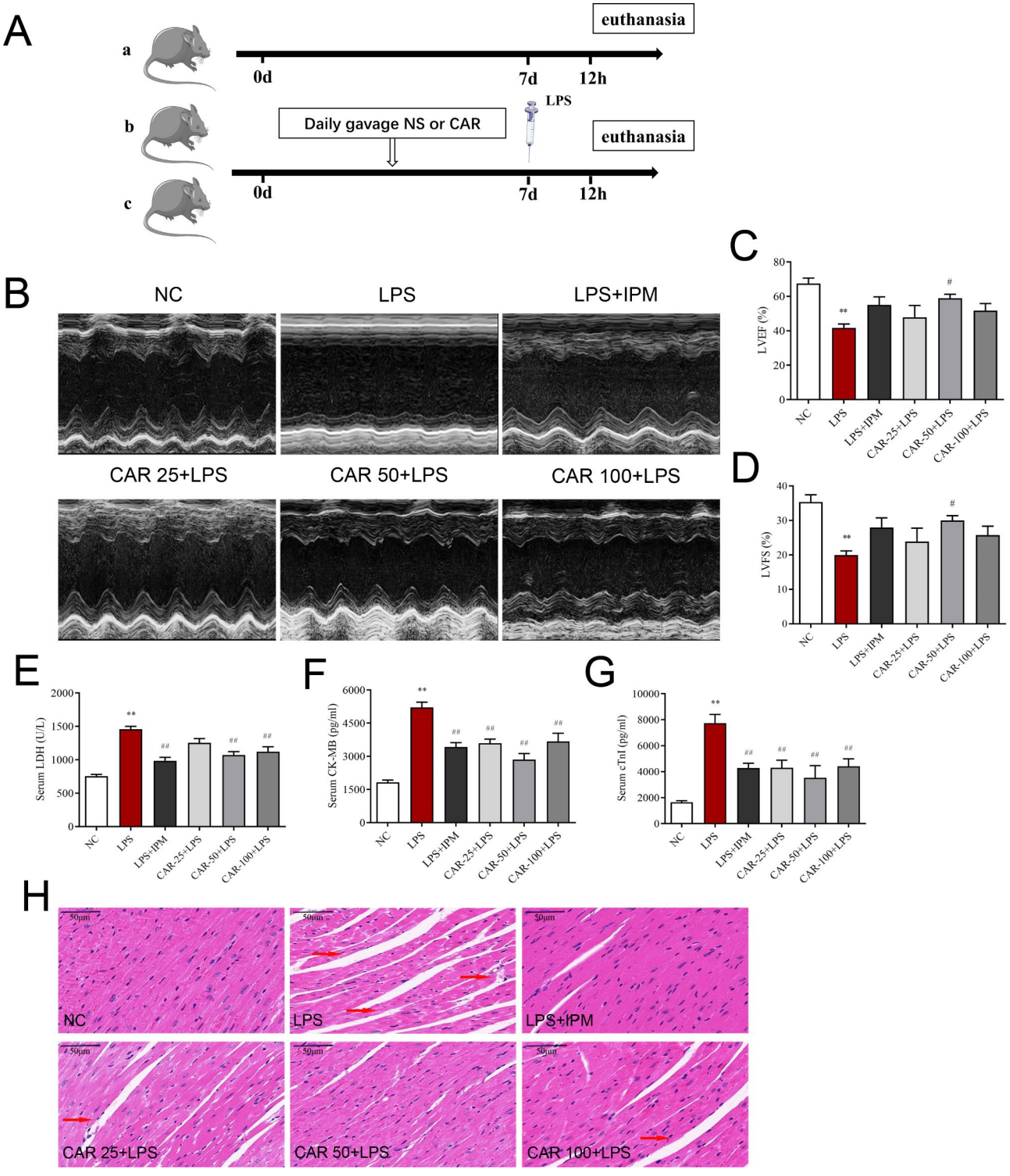

Fig. 1 CAR improved myocardial injury in LPS-injured mice. (**A**) Experimental design of this study. **a**: normal group, **b**: LPS-treated group, **c**: CAR-treated groups (25 mg/kg, 50 mg/kg and 100 mg/kg). (**B**) Cardiac function of M-mode echocardiography. (**C**) Left ventricular ejection fraction (LVEF). (**D**) Left ventricular fractional shortening (LVFS). Data are presented as mean ± SEM, $n = 5$ for each group. (**E**) Serum LDH level. (**F**) Serum CK-MB level. (**G**) Serum cTnI level. Data are presented as mean ± SEM, $n = 8$ for each group. (**H**) Representative HE-stained histological images. Arrows indicate cardiac tissues exhibited myofibril disorder. $^{**}P < 0.01$, compared with the NC group; $^{\#}P < 0.05$, $^{\#\#}P < 0.01$ compared with the LPS group. CAR, carvacrol; LPS, Lipopolysaccharide; LDH, lactate dehydrogenase; CK-MB, creatine kinase MB; cTnI, cardiac troponin I; NC, normal control

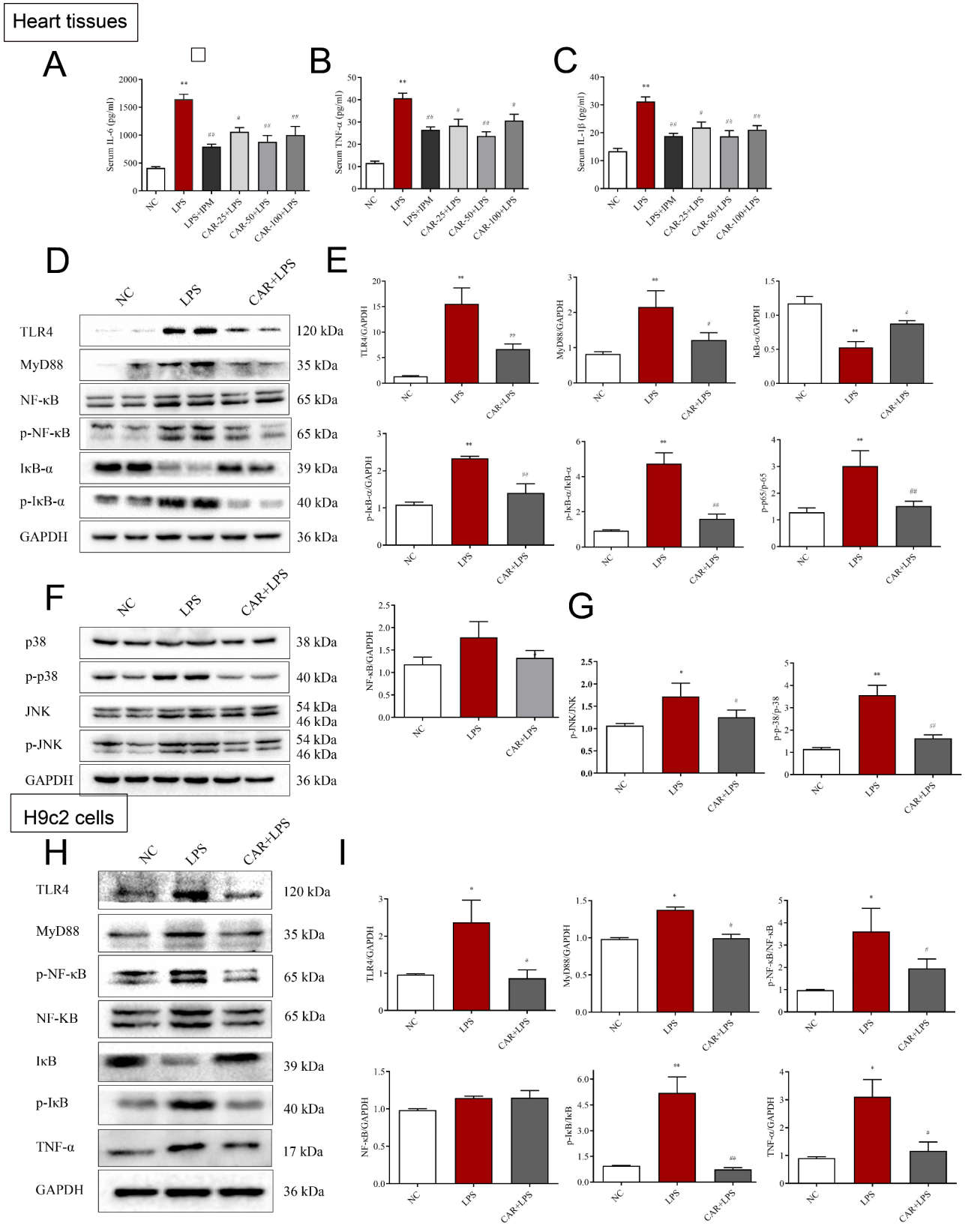

Fig. 2 (See legend on next page.)

(See figure on previous page.)

Fig. 2 CAR inhibited myocardial inflammation of LPS-induced injury in vivo and in vitro. (**A-C**) The serum level of TNF-α, IL-1β and IL-6. Data are presented as mean ± SEM, $n = 8$ in each group. (**D**) Representative Western blots images for TLR4, MyD88, NF-κB, p-NF-κB, IκB and p-IκB expression in heart tissues. (**E**) The quantitative analysis for TLR4, MyD88, NF-κB, p-NF-κB, IκB, p-IκB protein expression in heart tissues. (**F**) Representative Western blots images for p38, p-p38, JNK and p-JNK expression in heart tissues. (**G**) The quantitative analysis for p38, p-p38, JNK and p-JNK protein expression in heart tissues. (**H**) Representative Western blots images for TLR4, MyD88, NF-κB, p-NF-κB, IκB and p-IκB expression in H9c2 cells. (**I**) The quantitative analysis for TLR4, MyD88, NF-κB, p-NF-κB, IκB and p-IκB protein expression in H9c2 cells, GAPDH was used as the internal control. Data are presented as mean ± SEM, $n = 3$ for each group. $^{*}P < 0.05$, $^{**}P < 0.01$, compared with the NC group; $^{\#}P < 0.05$, $^{\#\#}P < 0.01$ compared with the LPS group. TNF-α, Tumor necrosis factor alpha; IL-1β, Interleukin-1β; IL-6, Interleukin-6; TLR4, Toll-like receptor4; MyD88, Myeloid differentiation factor 88; NF-κB, Nuclear factor-kappa B; IκB, Inhibitor of NF-κB; JNK, c-JunN-terminal kinase

visualized by a fluorescent microscope (Olympus, Tokyo, Japan).

TUNEL assay

Extensive DNA degradation is the signature of the late stage of apoptosis. TUNEL staining (horseradish peroxidase method) was conducted to detect apoptotic myocardial cells. All procedures were conducted in strict accordance with the manufacturer's instructions of the Wanlei Life Sciences Co., Ltd (Shenyang, China). Figures were immediately acquired at 400× magnification by a light microscope (Nikon, Tokyo, Japan). The proportion of TUNEL-positive cells was counted using Image-Pro Plus software (Version 6.0, Media Cybernetics, USA). Five different fields of each section were randomly selected for analysis, and the average value was taken as the final value of the sample. The apoptotic ratio was expressed as the percentage of the TUNEL-positive apoptotic myocytes to the total number of myocytes.

Western blot analysis

Samples of collected homogenized heart tissue or H9c2 cells were lysed and protein was extracted. Protein were transferred to nitrocellulose membranes (Bio-Rad Laboratories) after SDS/PAGE and blocked with 5% skim milk in 0.1% Tween 20/Tris Buffered Saline (TBST), the different bands of cell membrane were incubated by primary antibody against caspase-3 (1:1000), Bax (1:1000), Bcl-2 (1:1000), NF-κB (1:1000), phospho-NF-κB (1:1000), IκB (1:1000), phospho-IκB (1:1000), p38 (1:1000), phospho-p38 (1:1000), JNK (1:1000), phospho-JNK (1:1000), TLR4 (1:1000), MyD88 (1:1000), NLRP3 (1:1000), GSDMD (1:1000), Caspase-1 (1:1000), IL-1β (1:1000), IL-18 (1:1000), β-actin (1:2000) and GAPDH (1:2000) overnight at 4 °C. The membrane was then washed three times with TBST and incubated with a Horseradish peroxidase antibody. The band density of the films was detected by Imaging Lab system and images were analyzed using Image Lab software.

Statistical analysis

The statistical analysis was based on the ANOVA analysis and the Bonferroni multiple comparison posterior test and was performed using GraphPad Prism version 8.0 Software. All values were expressed as mean ± SEM. $^{*}P < 0.05$ was considered statistically significant.

Result

CAR improved myocardial injury in LPS-injured mice

As depicted in Fig. 1(B-D), the LVEF and LVFS in the LPS group were significantly reduced compared to the NC group. However, pretreatment with 50 mg/kg CAR significantly increased LVEF and LVFS. No significant difference was observed in the 25 mg/kg or 100 mg/kg CAR+LPS group. Serum cTnI, LDH, CK-MB are well-established markers used to assess myocardial damage. Figure 1(E-G) demonstrates that the levels of serum LDH, CK-MB and cTnI were significantly elevated in the LPS group compared to the NC group. Interestingly, these effects were effectively reversed by pretreatments with 50 mg/kg and 100 mg/kg CAR. As shown in Fig. 1(H), the HE staining of the myocardial tissues from NC mice did not reveal any significant histopathological changes, edema, or inflammation. However, after 24 h of LPS induction, the cardiac tissues exhibited myofibril disorder, muscle fiber swelling, necrosis, and infiltration of inflammatory cells. Importantly, treatment with CAR alleviated the aforementioned effects induced by LPS. These finding suggest that CAR treatment effectively mitigated LPS-induced myocardial dysfunction in mice.

CAR inhibited myocardial inflammation in LPS-injured cells and mice

Inflammatory cytokine production is regulated by multiple mechanisms, including TLR4 and its downstream signaling pathways, mitogen-activated protein kinase (MAPK) and nuclear factor κB (NF-κB) pathways [28]. LPS induces an inflammatory response, resulting in the release of several inflammatory cytokines including TNF-α, IL-1β and IL-6. As shown in Fig. 2(A-C), the expression of TNF-α, IL-1β and IL-6 was significantly elevated in mice subjected to LPS-induced injury. However, CAR treatment effectively suppressed these effects. The TLR4/MyD88/NF-κB signaling pathway plays a critical role in the regulation of the inflammatory response [29]. In this study, we analyzed the effects of CAR treatment on the TLR4, MyD88 and NF-kB pathway under LPS stimulation. Compared to the NC group, the expression levels of TLR4, MyD88, NF-κB, p-NF-κB and p-IκB proteins

in the myocardial tissue of LPS mice were significantly upregulated. In contrast, pretreatment with 50 mg/kg CAR significantly downregulated the protein expressions of TLR4, MyD88, as well as the phosphorylation levels of NF-κB and IκB. Meanwhile, a similar trend was also observed in LPS-treated H9c2 cells with CAR treatment. Also, we examined the MAPK signaling pathway. As shown in Fig. 2(F-G), compared to the normal control group, LPS significantly increased the phosphorylation levels of p38 and JNK proteins in myocardial tissue, however pretreatment with CAR significantly decreased p-p38 and JNK protein expression. These results suggest that CAR inhibits LPS-mediated inflammatory response-induced cardiac injury through the TLR4/NF-κB/MAPK signaling pathway.

CAR attenuated oxidative stress in LPS-injured cells and mice

LPS promotes cardiac mitochondrial ROS formation and oxidative stress, which further triggers cell membrane lipid peroxidation, mitochondrial dysfunction, intracellular calcium ion imbalance, etc., and ultimately leads to cardiomyocyte damage and death [5]. As shown in Fig. 3, ROS production was significantly increased both in LPS-treated H9c2 cells and cardiac tissues of mice. However, CAR treatment remarkably reversed the LPS-induced ROS accumulation. In addition, CAR treatment improved the reduction of SOD activity and decrease MDA levels in LPS mice. These results indicated that CAR treatment relieved myocardial injury by suppressing LPS-induced oxidative stress.

CAR alleviated myocardial apoptosis in LPS-mediated injury

Figure 4 showed that CAR treatment decreased the number of TUNEL-positive cells in the LPS group, indicating a low degree of apoptosis. To further investigate the molecular mechanism of CAR-mediated cardiac protection against sepsis, the protein levels of Bcl-2, Bax and caspase-3 were detected by Western blot. As expected, the expression of pro-apoptotic proteins Bax and Caspase-3 were apparently increased while the expression level of the anti-apoptotic protein Bcl-2 decreased in LPS mice. However, these effects were reversed by the CAR pretreatment. The above observation was also verified in H9c2 cells, as revealed by decreased protein expression of Bcl-2 and increased protein expression of Caspase-3 and Bax. The data implied that with CAR treatment alleviated LPS-induced cardiomyocyte apoptosis.

CAR inhibited pyroptosis in vitro model of LPS-induced injury

Finally, we examined the expression of NLRP3 inflammation proteins in vitro. As shown in Fig. 5, H9c2 cells exhibited a signature morphology of pyroptosis with cell swelling and membrane rupture after LPS challenge (red arrow). Moreover, CAR significantly downregulated the expression of NLRP3, GSDMD, Caspase-1, IL-1β and IL-18 proteins in the LPS-injured cells. These data suggest a role for CAR in protecting H9c2 cells against LPS injury-induced.

Discussion

Despite great efforts in basic research and clinical practice of SIMD in recent decades, the morbidity and mortality remain high [4]. The purpose of this study aims to find out the potential drugs for SIMD from natural drugs as well as to clarify the underlying mechanism. Terpenoids, especially monoterpenoids, have been shown to play a significant role in improving cardiovascular function and reducing risk factors for cardiovascular disease by protecting the vascular endothelium, antioxidizing, and scavenging free radicals [30]. CAR is a monoterpene phenolic compound with a wide range of applications due to its comprehensive pharmacological effects such as anti-inflammatory, antioxidant, antibacterial [27, 31–33]. In recent years, studies have shown that CAR plays an important role in sepsis-induced organ damage. Yan et al. [34] evidenced that the role of CAR in LPS-induced multi-organ damage, CAR significantly inhibited LPS-induced serum levels of the inflammatory cytokine IL-6 through modulation of the ERK1/2 signaling pathway in macrophages, thereby protecting mice from LPS-induced damage and ameliorating pathological damage in the liver, lungs, and heart. Joshi.et.al [35] demonstrated that CAR protects the cardiac from LPS-induced sepsis by decrease the levels of pro-inflammatory cytokines IL-1β and TNF-α in the cardiac, inhibited ROS production, and reduced NLRP3 inflammasome-mediated pyroptosis associated protein expression, in addition to activating autophagy. In our study, we demonstrated that CAR ameliorate LPS-induced myocardial dysfunction through the combination of TLR4/MYD88-mediated MAPK and NF-κB, and NLRP3-mediated pyroptosis pathways, which more comprehensively reveals and complements the mechanism of action of CAR in the treatment of SIMD.

Toll-like receptors (TLRs) are important recognition receptors in the process of inflammatory responses. TLR4, as the main receptor for LPS, can recognize Gram-negative bacteria [36, 37]. TLR4 binds to the downstream signaling ligand MyD88, then activates NF-κB, and forms the TLR4/MyD88/NF-κB axis, promoting the transcription and release of various inflammatory mediators, such as TNF-α, IL-1 and IL-6, the phenomenon known as cytokine storm. Due to the enormous role of the TLR4 signaling cascade, its extracellular and intracellular components are attractive therapeutic targets for

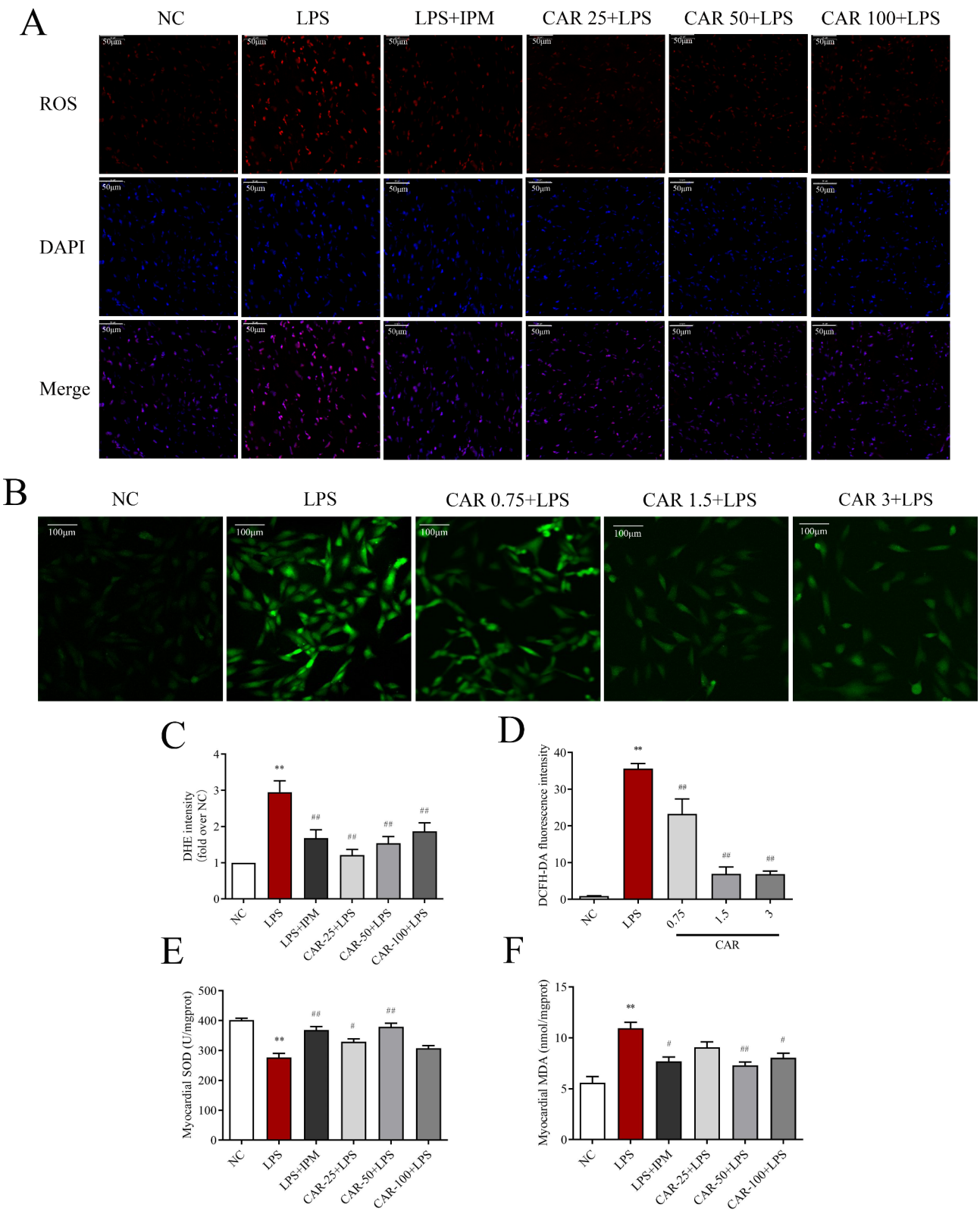

Fig. 3 CAR attenuated oxidative stress in LPS-induced injury in vivo and in vitro. (**A**) Representative images of ROS staining in heart tissues(200x). (**B**) Staining of intracellular ROS by DHE staining in H9c2 cells (400×). (**C**) DHE relative fluorescence in myocardium (%). (**D**) DCFH-DA fluorescence intensity in H9c2 cells (%). (**E-F**) SOD and MDA levels in cardiac tissue. Data are presented as mean ± SEM, $n = 8$ for each group. $^{*}P < 0.05$, $^{**}P < 0.01$, compared with the NC group; $^{\#}P < 0.05$, $^{\#\#}P < 0.01$ compared with the LPS group. ROS, reactive oxygen species; DHE, Dihydroethidium; SOD, superoxide dismutase; MDA, malondialdehyde

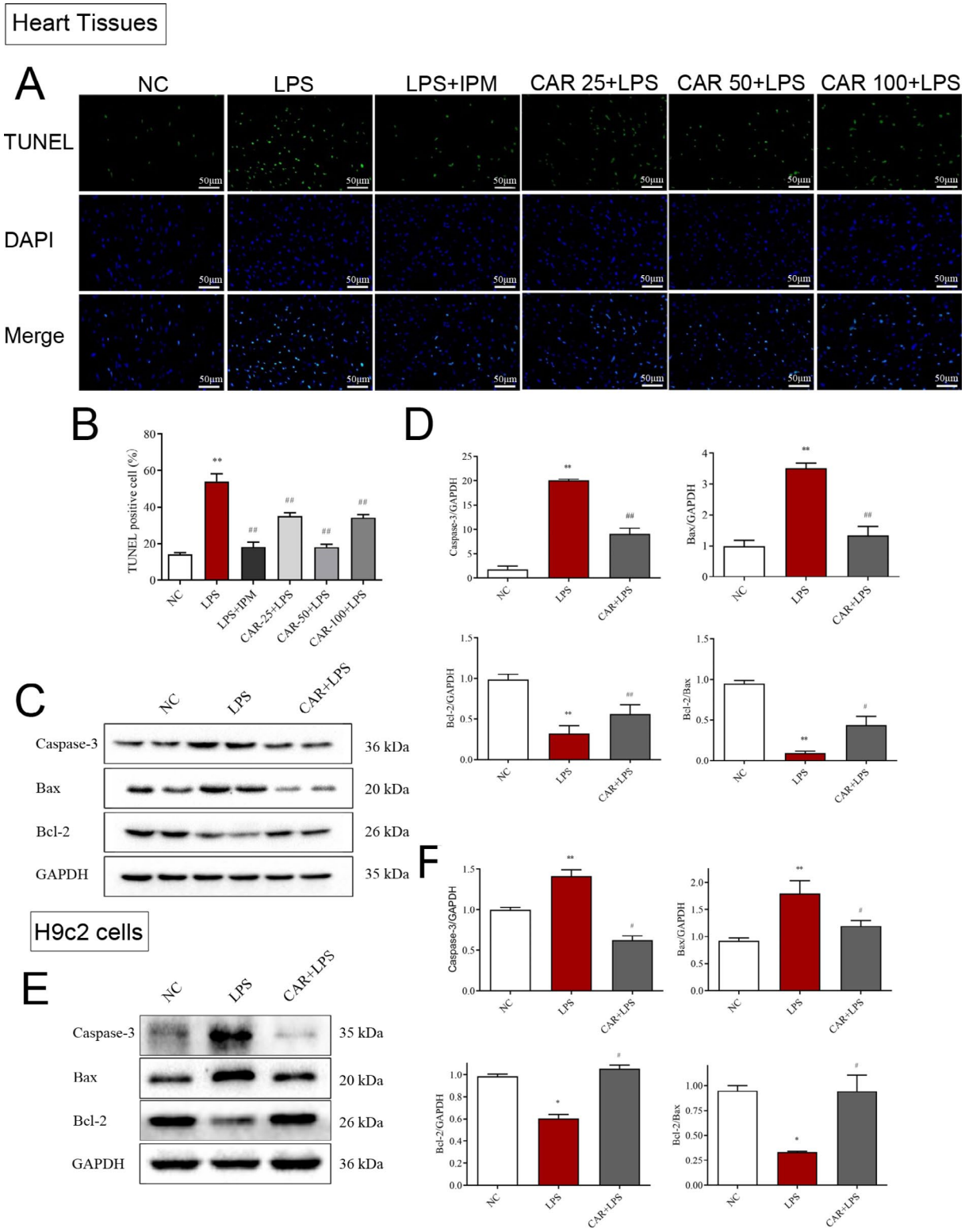

Fig. 4 CAR alleviated myocardial apoptosis in LPS-induced injury in vivo and in vitro. (**A**) TUNEL staining of each group. (**B**) TUNEL positive cell (%). (**C**) Representative Western blot images of Caspase-3, Bax and Bcl-2 in mice. (**D**) The protein levels of Caspase-3, Bax and Bcl-2 of each group. (**E**) Representative Western blots for Caspase-3, Bax and Bcl-2 expression in H9c2 cells. (**F**) The quantitative analysis for Caspase-3, Bax and Bcl-2 protein expression in H9c2 cells, GAPDH was used as the internal control. Data are presented as mean ± SEM, $n = 3$ for each group. $^{*}P < 0.05$, $^{**}P < 0.01$, compared with the NC group; $^{\#}P < 0.05$, $^{\#\#}P < 0.01$ compared with the LPS group. TUNEL, Terminal Deoxynucleotidyl Transferase-Mediated dUTP Nick End Labeling; Bax, BCL2-Associated X; Bcl-2, B-cell lymphoma-2

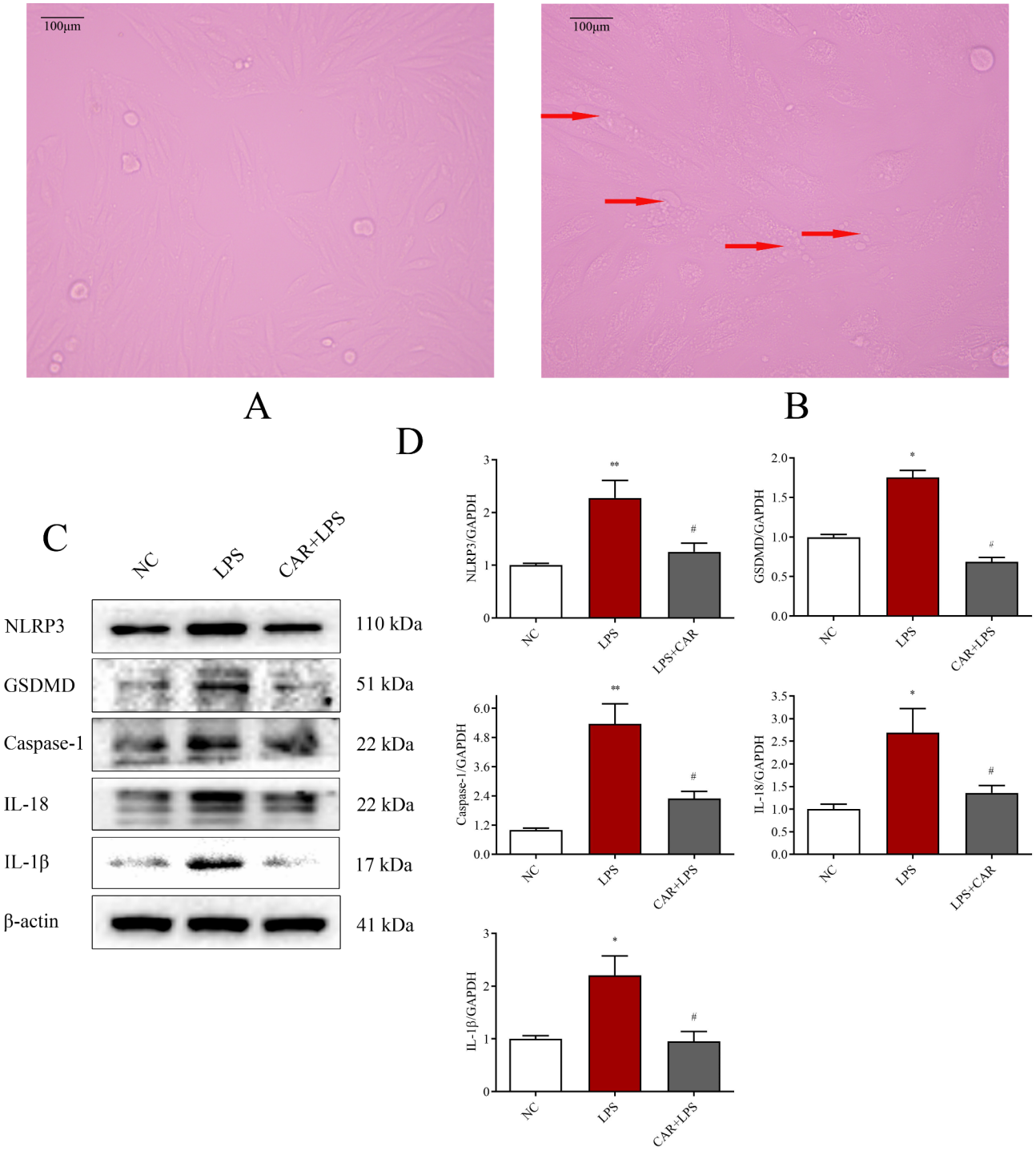

Fig. 5 CAR inhibited pyroptosis in LPS-induced cells. (**A**) Normal cultured H9c2 cells morphology. (**B**) Representative cellular morphology images of LPS-induced pyroptosis in H9c2 cells. (**C**) Representative Western blots images for NLRP3, GSDMD, Caspase-1, IL-1β and IL-18 expression in H9c2 cells. (**D**) The quantitative analysis for NLRP3, GSDMD, Caspase-1, IL-1β and IL-18 protein expression in H9c2 cells, β-actin was used as the internal control. Data are presented as mean ± SEM, $n = 3$ for each group. $^{*}P < 0.05$, $^{**}P < 0.01$, compared with the NC group; $^{\#}P < 0.05$, $^{\#\#}P < 0.01$ compared with the LPS group. NLRP3, NLR family pyrin domain containing 3; GSDMD, Gasdermin D; IL-18, Interleukin-18

acute injury, such as sepsis [10]. Under normal circumstances, NF-κB often occurs as a dimer (p65-p50), which binds to the inhibitory protein IκB to form an inactive trimer (p65-p50-IκB). When LPS invades, it can bind to TLR4 in the outer membrane and activate the NF-κB pathway through Pathogen-associated molecular patterns (PAMPs). IκB is phosphorylated and degraded by IκB kinase (IKK), and IκB is separated from NF-κB. Subsequently, activated NF-κB enters the nucleus and activates the transcription and expression of inflammatory mediators TNF-α, IL-1β, and IL-6 [38, 39]. This study found that LPS injection could activate the TLR4/NF-κB pathway. It was found that CAR could reverse the inflammatory injury caused by LPS and reduced the protein expression levels of TLR4 and NF-κB to exert a protective effect on septic myocardial injury.

LPS can not only activate the NF-KB signaling pathway, but also activate the mitogen-activated protein kinase (MAPK) signaling pathway [40, 41]. MAPK pathway is another important signal transduction pathway related to inflammation. ROS cause inflammatory responses by activating the MAPK signaling pathway, which in turn mediates the production of pro-inflammatory cytokines [42]. In our study, the expression levels of phosphorylated JNK and p38 protein in myocardial tissue were significantly increased, indicating that LPS injury can activate the cardiac MAPK signaling pathway, while pretreatment with CAR can significantly inhibit the phosphorylation of JNK and p38 in myocardial tissue. The above results suggest that the ability of CAR to suppress inflammation may be also attributed to the inhibition phosphorylation level of JNK and p38 proteins.

Apoptosis is important to maintain the normal growth and development of the body and protect the normal physiological metabolism of cells [43]. When stimulated by growth factors, hypoxia, oxidative stress, or DNA damage, apoptosis occurs, and disrupts the balance of the body, causing irreversible damage [43, 44]. Studies have shown that apoptosis exists in a variety of cardiovascular diseases, including sepsis and myocardial injury [8, 45]. To further investigate the mechanism of CAR-elicited amelioration effect on myocardial apoptosis, we focused on the levels of apoptosis-related proteins in mouse hearts. Bcl-2 acts as an inhibitor of apoptosis, while another family member Bax can promote apoptosis [46]. Our results showed that CAR pretreatment decreased Caspase-3 and Bax protein expressions and increased Bcl-2 protein expression in LPS-injured mice, suggesting the conspicuous anti-apoptosis activity of CAR against sepsis. Oxidative stress injury is also an important cause of myocardial injury in sepsis, and excessive ROS production causes damage to the heart, aggravate myocardial inflammation during sepsis, as well as directly destroy the structure of cardiomyocytes and promote apoptosis [5]. Therefore, inhibition of ROS production is essential for the treatment of sepsis. In our study, ROS levels were elevated in myocardial tissue and H9c2 cells after LPS treatment, and CAR reversed the associated changes.

The NLRP3 inflammasome can be activated by ROS-dependent signaling upon stimulation by PAMPs such as LPS [47]. ROS is important messengers for promoting inflammasome activation. They are also thought to play an important role in driving activation of the NLRP3/Caspase-1 complex and further leading to pyroptosis [48, 49]. In recent years, increasing studies have shown that the NLPR3 inflammasome/Caspase-1/IL-1β pathway may be involved in the occurrence of septic cardiac dysfunction due to excessive inflammatory response [50]. During pyroptosis, upstream stress signaling activates caspase-1, which directly leads to the GSDMS cleavage and the production of the C-terminal domain and the N-terminal product (GSDMD-N) that binds to phospholipid proteins on the cell membrane [51]. This alteration results in the formation of cell holes, the rupture of cells, the outflow of contents and the massive release of inflammatory factors, ultimately leading to cell death and the occurrence of surrounding inflammatory responses [52, 53]. In our study, the levels of IL-1β, IL-18 and pyroptosis-related proteins such as NLRP3, Caspase-1 and GSDMD were all increased by LPS challenge, while CAR pretreatment remitted the LPS-induced pyroptosis. Therefore, in addition to inhibiting inflammation and apoptosis, CAR can also inhibit LPS-induced myocardium injury by inhibiting the NLRP3/Caspase-1/GSDMD-mediated pyroptosis pathway.

In conclusion, this study demonstrated the protective effect of CAR against LPS-induced myocardial injury. Mechanistically, CAR significantly reduce LPS-induced inflammation, pyroptosis, apoptosis, and oxidative stress, which was partly related to the inhibition of TLR4/MyD88/NF-κB and NLRP3 inflammasome pathways. Our findings suggest that carvacrol may be a promising compound for the treatment of SIMD.

Abbreviations

CAR	Carvacrol
CK-MB	Creatine kinase MB
cTnI	Cardiac troponin I
H&E	Hematoxylin and Eosin
IκB	Inhibitor of NF-κB
IL-1β	Interleukin-1β
IL-6	Interleukin-6
GSDMD	Gasdermin D
LDH	Lactate dehydrogenase
LPS	Lipopolysaccharide
MAPKs	Mitogen-activated protein kinases
MDA	Malondialdehyde
MyD88	Myeloid differentiation factor 88
NLRP3	NLR family pyrin domain containing 3
NF-κB	Nuclear factor-kappa B
P-IκB	Phosphorylation-Inhibitor of NF-κB
SOD	Superoxide dismutase
SIMD	Sepsis-induced myocardial dysfunction

TNF-α	Tumor necrosis factor alpha
TLR	Toll-like receptor

Supplementary Information

The online version contains supplementary material available at https://doi.org/10.1186/s12950-024-00411-z.

Supplementary Material 1

Acknowledgements
The authors greatly appreciate professor Yang Yang of Northwest University for his guidance and supervision of this article.

Author contributions
Concept and design: LX, XY and SW. Data acquisition: XL and XL. Data interpretation/analysis: LX and HZ. Manuscript drafting: LX, SW, YL and YZ. Financial support: SW. All authors reviewed the manuscript.

Funding
This research was supported by the Shaanxi Key Laboratory of Biomedicine, China (Grant Number: 2018SZS41); and the Social Development of Shaanxi Province Key Project, China (Grant Number: 2021SF-152); and the Shaanxi Innovative Drug Research Center "Modern Chinese Medicine Research and Development" (Grant Number: 2022YWZX-PG-01). In addition,

Data availability
No datasets were generated or analysed during the current study.

Declarations

Ethics approval and consent to participate
All the animal experiments procedures were performed with the approval of the Air Force Military Medical University (No. 20191206).

Consent for publication
Not applicable.

Competing interests
The authors declare no competing interests.

Received: 15 November 2023 / Accepted: 16 September 2024
Published online: 15 November 2024

References

1. Singer M, Deutschman CS, Seymour CW, Shankar-Hari M, Annane D, Bauer M, Bellomo R, Bernard GR, Chiche JD, Coopersmith CM, Hotchkiss RS, Levy MM, Marshall JC, Martin GS, Opal SM, Rubenfeld GD, van der Poll T. JL Vincent, DC Angus. The Third International Consensus definitions for Sepsis and septic shock (Sepsis-3). JAMA. 2016;315:801–10.
2. Lv X, Wang H. Pathophysiology of sepsis-induced myocardial dysfunction. Mil Med Res. 2016;3:30.
3. Prescott HC, Angus DC. Enhancing recovery from Sepsis: a review. JAMA. 2018;319:62–75.
4. Hollenberg SM, Singer M. Pathophysiology of sepsis-induced cardiomyopathy. Nat Rev Cardiol. 2021;18:424–34.
5. Lin Y, Xu Y, Zhang Z. Sepsis-Induced Myocardial Dysfunction (SIMD): the pathophysiological mechanisms and therapeutic strategies targeting Mitochondria. Inflammation. 2020;43:1184–200.
6. Khosrojerdi A, Soudi S, Hosseini AZ, Khaligh SG, Hashemi SM. The combination of mesenchymal stem cell- and hepatocyte-derived exosomes, along with imipenem, ameliorates inflammatory responses and liver damage in a sepsis mouse model. Life Sci. 2023;326:121813.
7. Avlas O, Fallach R, Shainberg A, Porat E, Hochhauser E. Toll-like receptor 4 stimulation initiates an inflammatory response that decreases cardiomyocyte contractility. Antioxid Redox Signal. 2011;15:1895–909.
8. Li N, Zhou H, Wu H, Wu Q, Duan M, Deng W, Tang Q. STING-IRF3 contributes to lipopolysaccharide-induced cardiac dysfunction, inflammation, apoptosis and pyroptosis by activating NLRP3. Redox Biol. 2019;24:101215.
9. Maldonado RF, Sá-Correia I, Valvano MA. Lipopolysaccharide modification in Gram-negative bacteria during chronic infection. FEMS Microbiol Rev. 2016;40:480–93.
10. Kuzmich NN, Sivak KV, Chubarev VN, Porozov YB, Savateeva-Lyubimova TN, Peri F. TLR4 signaling pathway modulators as potential therapeutics in inflammation and Sepsis. Vaccines (Basel). 2017;5.
11. Faria SS, Costantini S, de Lima VCC, de Andrade VP, Rialland M, Cedric R, Budillon A, Magalhães KG. NLRP3 inflammasome-mediated cytokine production and pyroptosis cell death in breast cancer. J Biomed Sci. 2021;28:26.
12. An N, Gao Y, Si Z, Zhang H, Wang L, Tian C, Yuan M, Yang X, Li X, Shang H, Xiong X, Xing Y. Regulatory mechanisms of the NLRP3 Inflammasome, a Novel Immune-inflammatory marker in Cardiovascular diseases. Front Immunol. 2019;10:1592.
13. Dai S, Ye B, Chen L, Hong G, Zhao G, Lu Z. Emodin alleviates LPS-induced myocardial injury through inhibition of NLRP3 inflammasome activation. Phytother Res. 2021;35:5203–13.
14. Sharifi-Rad M, Varoni EM, Iriti M, Martorell M, Setzer WN, Del Mar M, Contreras B, Salehi A, Soltani-Nejad S, Rajabi M, Tajbakhsh J. Sharifi-Rad. Carvacrol and human health: a comprehensive review. Phytother Res. 2018;32:1675–87.
15. Boskabady MH, Alitaneh S, Alavinezhad A. Carum copticum L.: a herbal medicine with various pharmacological effects. Biomed Res Int. 2014;2014:569087.
16. Suntres ZE, Coccimiglio J, Alipour M. The bioactivity and toxicological actions of carvacrol. Crit Rev Food Sci Nutr. 2015;55:304–18.
17. Khan F, Khan I, Farooqui A, Ansari IA. Carvacrol Induces Reactive Oxygen Species (ROS)-mediated apoptosis along with cell cycle arrest at G(0)/G(1) in human prostate Cancer cells. Nutr Cancer. 2017;69:1075–87.
18. Khan F, Singh VK, Saeed M, Kausar MA, Ansari IA. Carvacrol Induced Program Cell death and cell cycle arrest in androgen-independent human prostate Cancer cells via inhibition of Notch Signaling. Anticancer Agents Med Chem. 2019;19:1588–608.
19. Liu SD, Song MH, Yun W, Lee JH, Kim HB, Cho JH. Effect of carvacrol essential oils on immune response and inflammation-related genes expression in broilers challenged by lipopolysaccharide. Poult Sci. 2019;98:2026–33.
20. Guan X, Li X, Yang X, Yan J, Shi P, Ba L, Cao Y, Wang P. The neuroprotective effects of carvacrol on ischemia/reperfusion-induced hippocampal neuronal impairment by ferroptosis mitigation. Life Sci. 2019;235:116795.
21. De Vincenzi M, Stammati A, De Vincenzi A, Silano M. Constituents of aromatic plants: carvacrol. Fitoterapia. 2004;75:801–4.
22. Zhao W, Deng C, Han Q, Xu H, Chen Y. Carvacrol may alleviate vascular inflammation in diabetic db/db mice. Int J Mol Med. 2020;46:977–88.
23. Chen Y, Ba L, Huang W, Liu Y, Pan H, Mingyao E, Shi P, Wang Y, Li S, Qi H, Sun H, Cao Y. Role of carvacrol in cardioprotection against myocardial ischemia/reperfusion injury in rats through activation of MAPK/ERK and Akt/eNOS signaling pathways. Eur J Pharmacol. 2017;796:90–100.
24. Yu W, Liu Q, Zhu S. Carvacrol protects against acute myocardial infarction of rats via anti-oxidative and anti-apoptotic pathways. Biol Pharm Bull. 2013;36:579–84.
25. Jafarinezhad Z, Rafati A, Ketabchi F, Noorafshan A, Karbalay-Doust S. Cardioprotective effects of curcumin and carvacrol in doxorubicin-treated rats: stereological study. Food Sci Nutr. 2019;7:3581–8.
26. El-Sayed SM el, Mansour AM, Abdul-Hameed MS. Thymol and Carvacrol Prevent Doxorubicin-Induced cardiotoxicity by abrogation of oxidative stress, inflammation, and apoptosis in rats. J Biochem Mol Toxicol. 2016;30:37–44.
27. Marconi GD, Della Rocca Y, Fonticoli L, Guarnieri S, Carradori S, Rajan TS, Pizzicannella J, Diomede F. The Beneficial Effect of Carvacrol in HL-1 cardiomyocytes treated with LPS-G: anti-inflammatory pathway investigations. Antioxid (Basel). 2022;11.
28. Ning L, Rong J, Zhang Z, Xu Y. Therapeutic approaches targeting renin-angiotensin system in sepsis and its complications. Pharmacol Res. 2021;167:105409.
29. Zhang Y, Liang X, Bao X, Xiao W, Chen G. Toll-like receptor 4 (TLR4) inhibitors: current research and prospective. Eur J Med Chem. 2022;235:114291.
30. Saljoughian S, Roohinejad S, Bekhit AEA, Greiner R, Omidizadeh A, Nikmaram N, Khaneghah AM. The effects of food essential oils on cardiovascular diseases: a review. Crit Rev Food Sci Nutr. 2018;58:1688–705.
31. Riaz M, Al Kury LT, Atzaz N, Alattar A, Alshaman R, Shah FA, Li S. Carvacrol alleviates Hyperuricemia-Induced oxidative stress and inflammation by modulating the NLRP3/NF-κB Pathwayt. Drug Des Devel Ther. 2022;16:1159–70.

32. Wijesundara NM, Lee SF, Cheng Z, Davidson R, Rupasinghe HPV. Carvacrol exhibits rapid bactericidal activity against Streptococcus pyogenes through cell membrane damage. Sci Rep. 2021;11:1487.
33. Wijesundara NM, Lee SF, Davidson R, Cheng Z, Rupasinghe HPV. Carvacrol suppresses inflammatory biomarkers production by Lipoteichoic Acid- and peptidoglycan-stimulated human tonsil epithelial cells. Nutrients. 2022;14.
34. Yan C, Kuang W, Jin L, Wang R, Niu L, Xie C, Ding J, Liao Y, Wang L, Wan H, Ma G. Carvacrol protects mice against LPS-induced sepsis and attenuates inflammatory response in macrophages by modulating the ERK1/2 pathway. Sci Rep. 2023;13:12809.
35. Joshi S, Kundu S, Priya VV, Kulhari U, Mugale MN, Sahu BD. Anti-inflammatory activity of carvacrol protects the heart from lipopolysaccharide-induced cardiac dysfunction by inhibiting pyroptosis via NLRP3/Caspase1/Gasdermin D signaling axis. Life Sci. 2023;324:121743.
36. Guo S, Guo L, Fang Q, Yu M, Zhang L, You C, Wang X, Liu Y, Han C. Astaxanthin protects against early acute kidney injury in severely burned rats by inactivating the TLR4/MyD88/NF-κB axis and upregulating heme oxygenase-1. Sci Rep. 2021;11:6679.
37. Li Y, Wang N, Ma Z, Wang Y, Yuan Y, Zhong Z, Hong Y, Zhao M. Lipoxin A4 protects against paraquat–induced acute lung injury by inhibiting the TLR4/MyD88–mediated activation of the NF–κB and PI3K/AKT pathways. Int J Mol Med. 2021;47.
38. Lawrence T. The nuclear factor NF-kappaB pathway in inflammation. Cold Spring Harb Perspect Biol. 2009;1:a001651.
39. Hayden MS, Ghosh S. Shared principles in NF-kappaB signaling. Cell. 2008;132:344–62.
40. Shyni GL, Renjitha J, Raghu BSSKG. Zerumin A attenuates the inflammatory responses in LPS-stimulated H9c2 cardiomyoblasts. J Biochem Mol Toxicol. 2021;35:1–11.
41. Zhang J, Wang M, Ye J, Liu J, Xu Y, Wang Z, Ye D, Zhao M, Wan J. The anti-inflammatory mediator resolvin E1 protects mice against Lipopolysaccharide-Induced Heart Injury. Front Pharmacol. 2020;11:203.
42. Kumar V. Toll-like receptors in sepsis-associated cytokine storm and their endogenous negative regulators as future immunomodulatory targets. Int Immunopharmacol. 2020;89:107087.
43. Li Y, Liu X. The inhibitory role of Chinese materia medica in cardiomyocyte apoptosis and underlying molecular mechanism. Biomed Pharmacother. 2019;118:109372.
44. Li P, Dong X-R, Zhang B, Zhang X-T, Liu J-Z, Ma D-S, Ma L. Molecular mechanism and therapeutic targeting of necrosis, apoptosis, pyroptosis, and autophagy in cardiovascular disease. Chin Med J. 2021;134.
45. Li P, Dong XR, Zhang B, Zhang XT, Liu JZ, Ma DS, Ma L. Molecular mechanism and therapeutic targeting of necrosis, apoptosis, pyroptosis, and autophagy in cardiovascular disease. Chin Med J (Engl). 2021;134:2647–55.
46. Peña-Blanco A, García-Sáez AJ. Bax, Bak and beyond - mitochondrial performance in apoptosis. FEBS J. 2018;285:416–31.
47. Song W, Wei L, Du Y, Wang Y, Jiang S. Protective effect of ginsenoside metabolite compound K against diabetic nephropathy by inhibiting NLRP3 inflammasome activation and NF-κB/p38 signaling pathway in high-fat diet/streptozotocin-induced diabetic mice. Int Immunopharmacol. 2018;63:227–38.
48. Liu Q, Zhang D, Hu D, Zhou X, Zhou Y. The role of mitochondria in NLRP3 inflammasome activation. Mol Immunol. 2018;103:115–24.
49. Yu X, Lan P, Hou X, Han Q, Lu N, Li T, Jiao C, Zhang J, Zhang C, Tian Z. HBV inhibits LPS-induced NLRP3 inflammasome activation and IL-1β production via suppressing the NF-κB pathway and ROS production. J Hepatol. 2017;66:693–702.
50. Garnacho-Montero J, Palacios-García I, Díaz-Martín A, Gutiérrez-Pizarraya A, López-Sánchez JM. EA Gómez, MD Cordero. Sequential changes of NLRP3 inflammasome activation in Sepsis and its relationship with death. Shock. 2020;54:294–300.
51. Burdette BE, Esparza AN, Zhu H, Wang S. Gasdermin D in pyroptosis. Acta Pharm Sin B. 2021;11:2768–82.
52. Burzynski LC, Clarke MCH. Death is coming and the clot thickens, as pyroptosis feeds the fire. Immunity. 2019;50:1339–41.
53. McKenzie BA, Mamik MK, Saito LB, Boghozian R, Monaco MC, Major EO, Lu JQ, Branton WG, Power C. Caspase-1 inhibition prevents glial inflammasome activation and pyroptosis in models of multiple sclerosis. Proc Natl Acad Sci U S A. 2018;115:E6065–74.

Publisher's note